

Synthesis, characterization and thermolysis studies on triazole and tetrazole based high nitrogen content high energy materials

R. Sivabalan*, M. Anniyappan, S.J. Pawar, M.B. Talawar, G.M. Gore,
S. Venugopalan, B.R. Gandhe

High Energy Materials Research Laboratory, Pune 411 021, India

Received 15 December 2005; received in revised form 7 March 2006; accepted 10 March 2006

Available online 25 April 2006

Abstract

This paper reports the synthesis, characterisation and thermolysis studies of hydrazinium azotetrazolate (HAZ) and 1,1'-dinitro-3,3'-azo-1,2,4-triazole (N-DNAT). TGA and DSC results suggested that HAZ decomposes in the range of 150–180 °C and N-DNAT in the range of 160–170 °C, respectively. The pattern of decomposition of HAZ dihydrate and N-DNAT has been predicted with the help of pyrolysis GC/MS technique and a probable decomposition mechanism has been proposed. The theoretically predicted performance data suggests the potential nature of HAZ and N-DNAT for their use in propellant/explosive as well as in gas generator formulations.

© 2006 Elsevier B.V. All rights reserved.

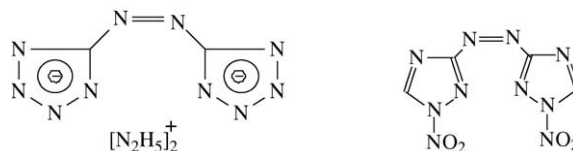
Keywords: High nitrogen content high energy materials (HNC-HEMs); Hydrazinium azotetrazolate; Dinitroazotriazole; Synthesis; Thermolysis

1. Introduction

The concept of new class of high nitrogen content high energy materials (HNC-HEMs) has evinced great interest [1–8] during recent time as an energetic component of propellants. Presence of N–N and C–N bonds in HNC compounds confers positive heat of formation on them. Further, HNC-HEMs produce more nitrogen gas per gramme than most of the HEMs, resulting in inherently cooler combustion products, which is an attractive feature for gun propellants and gas generators [3]. Low percentage of carbon and hydrogen in these compounds reduces the proportion of oxidized combustion products in comparison to conventional HEMs, resulting in formation of low mean molecular weight combustion products like methane [4]. These compounds are reported to have a combination of high positive heat of formation and insensitivity.

This paper reports the synthesis and characterization of two potential high nitrogen compounds with the objective of generating additional data on this class of compounds in view of their increasing importance in the field of HEMs. The

present work aims at the development of safer and cleaner HEMs for futuristic applications. These compounds have better insensitivity towards accidental exposure during development, processing, storage and transportation:



Hydrazinium azotetrazolate (HAZ) [9,10] and 1,1'-dinitro-3,3'-azo-1,2,4-triazole (N-DNAT) [11–13] are known potential HNC-HEMs. The reported heat of formation for hydrazinium azotetrazolate (HAZ) [9] and 1,1'-dinitro-3,3'-azo-1,2,4-triazole (N-DNAT) [11] are +206 and +94.4 kcal/mol, respectively. Precursors such as barium azotetrazolate, hydrazinium azotetrazolate dihydrate, 3, 3'-azo-1,2,4-triazole (ATA) and products were characterized by spectroscopic methods. Thermal studies were carried out to understand decomposition pattern and hyphenated TG-FT-IR studies were conducted to identify the gaseous products of decomposition of synthesized compounds. The decomposition pattern of HAZ and N-DNAT has been studied by pyrolysis gas chromatography mass spectrometry (P-GC/MS) technique and a probable decomposition pathway has been proposed. The trends obtained are discussed on the lines

* Corresponding author. Tel.: +91 20 25869303; fax: +91 20 25869316.
E-mail address: rsivabalan2001@yahoo.co.in (R. Sivabalan).

of reported literature. The theoretical performance data of these compounds also generated.

Another interesting high nitrogen compound namely, 3,6-diazido-1,2,4,5-tetrazine (DATz) has also been synthesized by modifying the reported method [14]. Since DATz exploded during the characterization studies and it decomposes during storage for long time, further work on DATz was stopped.

2. Experimental

2.1. Materials

All the reagents and chemicals used in the present study were of AR grade and used as such. The IR spectra were recorded on Perkin-Elmer FT-IR-1600 spectrophotometer in KBr matrix. ¹H NMR spectra were recorded on 300 MHz Varian instrument at 30 °C with TMS as an internal standard. DSC studies were undertaken on a Perkin-Elmer DSC-7 instrument operating at different heating rate (5, 10, 15 and 20 °C/min) in nitrogen atmosphere with 1 mg of sample. The thermal decomposition studies were also undertaken on thermo gravimetric/simultaneous differential thermal analyzer (TG/SDTA) of Mettler Toledo make (8551). FT-IR of decomposition products was recorded on Bruker (EQUINOX-55) make instrument coupled with TG. The crystal morphology has been studied by scanning electron microscope (SEM) instrument of Philips Icon make.

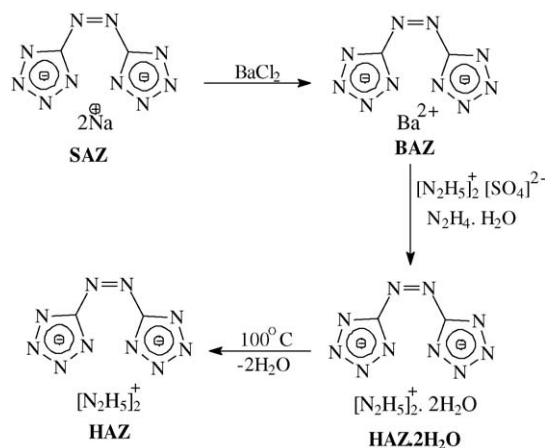
Thermal decomposition products of HAZ dihydrate and N-DNAT have been identified by pyrolysis GC/MS technique. Pyrolysis of the sample was carried out with CDS model 1000 pyroprobe (coil probe, sample taken in quartz capillary tube) at 800 °C for 15 s under helium (He) atmosphere. Pyrolyzer was connected to a gas chromatography (Perkin-Elmer, Clarus 500) with split/split less injector. Helium was used as carrier gas at a flow rate of 1 mL/min (held pressure 10 psi). Elite-5 capillary column (30 m × 0.25 mm × 0.25 μm) was used (stationary phase: cross bonded diphenyl, 5% ;dimethyl polysiloxane, 95%) for the study. Perkin-Elmer turbomatrix quadruple mass spectrometer (Turbo Mass) coupled with GC via heated (at 200 °C) interface was used for the pyrolysis study.

The sensitivity to impact stimuli was determined by applying standard staircase method using a 2 kg drop weight and the results are reported in terms of height for 50% probability of explosion (*h*_{50%}) of the sample [15]. Figure of insensitivity (F of I) was computed by using tetryl (composition exploding, CE), as reference. The friction sensitivity of the compound was determined on Julius Peter's apparatus till there was no explosion/ignition in five consecutive test samples at that weight.

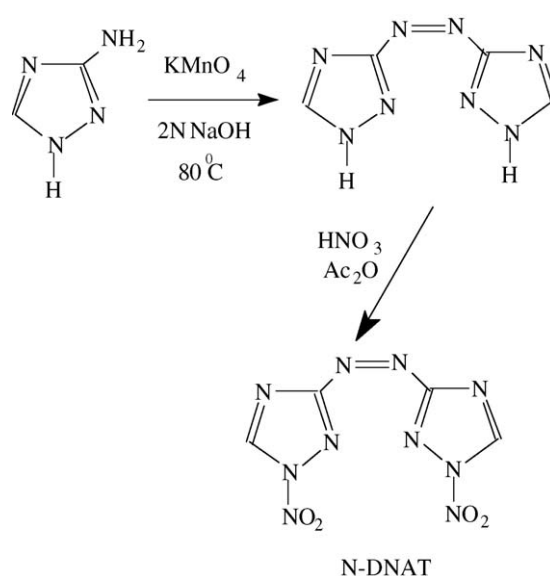
Hydrazinium azotetrazolate (HAZ) [9,10], 1,1'-dinitro-3,3'-azo-1,2,4-triazole (N-DNAT) [11–13] and 3,6-diazido-1,2,4,5-tetrazine (DATz) [14] were synthesized by following the reported procedures and depicted in Schemes 1–3.

2.2. Synthesis

Sodium azotetrazolate pentahydrate (SAZ)—a key synthon for the preparation of wide variety of energetic azotetrazolates has been synthesized [7]. The synthesised SAZ has been utilized



Scheme 1. Synthesis of hydrazinium azotetrazolate.



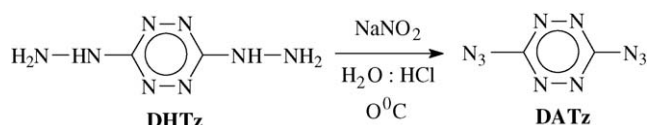
Scheme 2. Synthesis of 1,1'-dinitro-3,3'-azo-1,2,4-triazole (N-DNAT).

for the preparation of another important precursor known as barium azotetrazolate pentahydrate (BAZ) and followed by to hydrazinium azotetrazolate (Scheme 1).

2.2.1. Hydrazinium azotetrazolate (HAZ)

SAZ (10 g, 0.033 mol) was dissolved in 250 mL of water with stirring. Solid barium chloride dihydrate (8.05 g, 0.033 mol) was added to the above solution and stirred vigorously for 30 min to obtain BAZ.5H₂O (1). The yellow solid precipitated (11.5 g, yield = 88%) was filtered and dried at 70 °C.

BAZ.5H₂O (10 g, 0.0255 mol) was taken in 250 mL of water and hydrazinium sulfate (6.05 g, 0.025 mol) was added to the above solution with stirring at 25–30 °C followed by the drop



Scheme 3. Synthesis of 3,6-diazido-1,2,4,5-tetrazine (DATz).

wise addition of hydrazine hydrate (1.25 g, 0.025 mol). Stirring was continued for 1 h and the precipitate formed was removed by filtration. The filtrate was distilled to one third and kept overnight for crystallization. The yellow needle shaped solid formed was filtered and air-dried to get hydrazinium azotetrazolate dihydrate (5.5 g, 80%). Further, hydrazinium azotetrazolate dihydrate was dried in a furnace at 100 °C for 18 h to get anhydrous hydrazinium azotetrazolate (4.26 g).

2.2.2. Synthesis of 1,1'-dinitro-3,3'-azo-1,2,4-triazole (N-DNAT)

3-Amino-1,2,4-triazole (8.4 g, 0.1 mol) was dissolved in 100 mL of NaOH (2N) solution with constant stirring and the solution was cooled. Potassium permanganate (10.59 g, 0.06 mol) was added gradually to the cooled solution. After complete dissolution, the reaction mixture was heated to ~60 °C and additional potassium permanganate was added until the solution remains green. Sodium bisulfite solution was added to the hot solution to destroy the unreacted potassium permanganate and the mixture was filtered to obtain ATA as yellowish precipitate by adding concentrated HCl to the hot filtrate. ATA was filtered, thoroughly washed with water and dried (Scheme 2).

ATA (0.6 g, 0.0037 mol) was added slowly to a mixture of 98% nitric acid (2.1 mL, 0.05 mol) and acetic anhydride (4.7 mL, 0.05 mol) at 0 °C. The reaction mixture was stirred at ~6 °C for 1 h and poured into crushed ice and kept overnight. The solid thus obtained is washed with water and recrystallized from acetone (yield 56%).

2.2.3. Synthesis of 3,6-diazido-1,2,4,5-tetrazine (DATz)

3,6-Dihydrazino-1,2,4,5-tetrazine (0.5 g, 0.0035 mol) was dissolved in 30 mL of conc. HCl at 0 °C. After complete dissolution, sodium nitrite (0.483 g, 0.007 mol) in 5 mL of water was added drop wise with constant stirring (Scheme 3). The reaction mixture was filtered immediately to obtain 3,6-diazido-1,2,4,5-tetrazine as orange colour precipitate and washed with water and dried in vacuum (0.425 g, 74%).

The synthesized HNC-HEMs were characterized by spectroscopic and thermal methods (Table 1). The synthesized compounds have been scaled up to 10 g/batch level.

3. Results and discussion

3.1. Spectral studies

The UV spectrum of HAZ showed absorption bands in ultra-violet and visible region at 308 and 426 nm due to the $\pi \rightarrow \pi^*$ and $n \rightarrow \pi^*$ electronic transitions and N-DNAT showed at 326 and 430 nm due to the same transitions. The IR spectrum of HAZ showed an asymmetric ring stretching (C–N) vibration at 1386 cm^{-1} and an asymmetric stretching mode of the azo group at 774 cm^{-1} , in addition to peaks attributable to hydrazinium groups 3318 and 3210 and 1684 and 1614 cm^{-1} corresponding to stretching and bending frequencies, respectively. N-DNAT showed absorption in IR spectrum at 3136 cm^{-1} stretching due to two rings (C–H) and at 1500 and 1318 cm^{-1} attributable to asymmetric and symmetric stretching of NO_2 group. In proton NMR spectrum of HAZ, the protons of hydrazinium group resonated at δ 6.65 (bs, $-\text{N}_2\text{H}_5$) whereas the two protons present in the triazole ring of N-DNAT appeared at δ 9.99 (s, 2H, C–H). In ^{13}C NMR spectrum, two carbon atoms of the azotetrazolate ring appeared at δ 173.6. In the case N-DNAT, two carbon atoms bonded with hydrogen (C–H) resonated at δ 143 and the C–N carbon atoms appeared at δ 163. The elemental analyses data of HAZ, HAZ dihydrate and N-DAT are in good agreement with calculated values present in brackets.

3.2. SEM studies

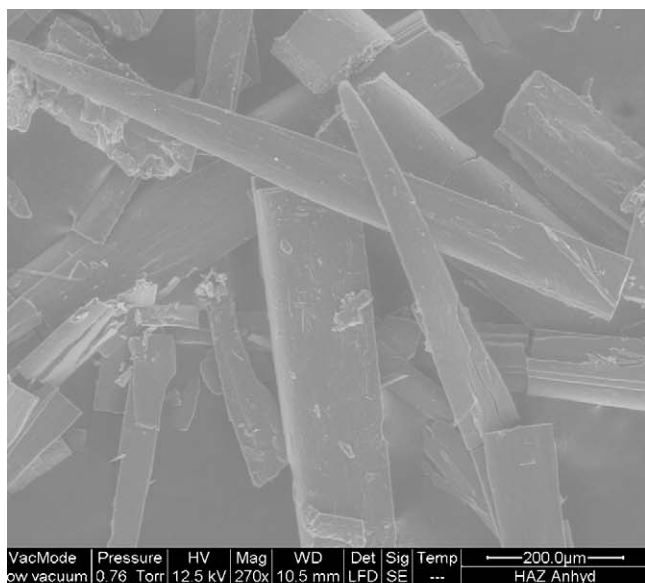
The surface morphology studies showed that anhydrous HAZ (Fig. 1) as well as HAZ dihydrate (Fig. 2) have rod type crystal morphology while N-DNAT (Fig. 3) has plate type crystal morphology with sharp edges. This may be the reason for the sensitive nature of N-DNAT to mechanical stimuli.

3.3. Thermal studies

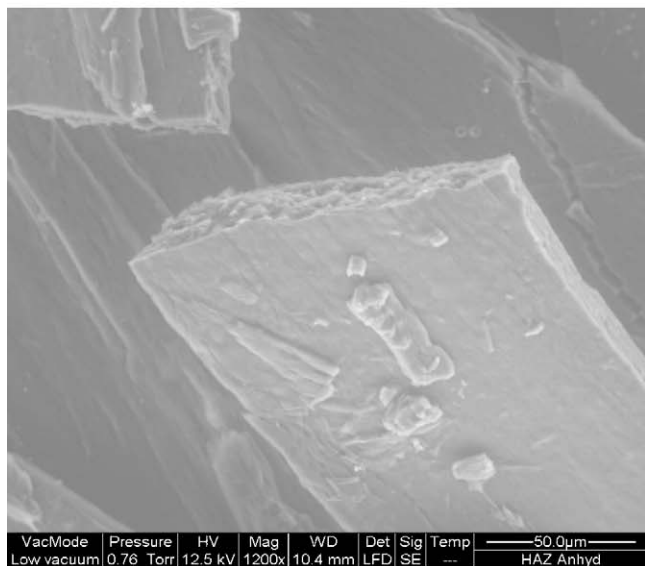
DSC results revealed that HAZ dihydrate (Fig. 4) showed an endothermic peak in the temperature range 85–105 °C due to the dehydration followed by an exothermic decomposition at 177–193 °C with the heat evolution of 885–1626 J/g at the heat-

Table 1
Physico-chemical properties of HNC-HEMs

Technique	HAZ	N-DNAT
Crystal morphology	Rod shaped	Plate shaped
UV (nm)	426 ($n \rightarrow \pi^*$), 308 ($\pi \rightarrow \pi^*$)	430 ($n \rightarrow \pi^*$), 326 ($\pi \rightarrow \pi^*$)
IR (cm^{-1})	3318, 3210, 1684(N_2H_5), 1386 (C–N), 774 (N=N)	3136 (C–H), 1500, 1318 (NO_2)
^1H NMR (δ)	6.65 (bs, 5H, N_2H_5)	9.99 (s, 2H, C–H)
^{13}C NMR (δ)	173.6	143 (C–H), 163 (C–N)
Elemental analysis (%) (calculated values are given in parentheses)	C: 10.22 (10.43), H: 4.43 (4.38), N: 85.72 (85.217)	C: 18.38 (18.90), H: 0.50 (0.79), N: 56.32 (55.12)
DSC (°C)		
T_i	168	159
T_m	188 (exo)	172 (exo)
T_f	200	178
ΔH (J/g)	1650	1368
TG (°C, mass loss %)	150–185 (77%)	160–180 (85%)

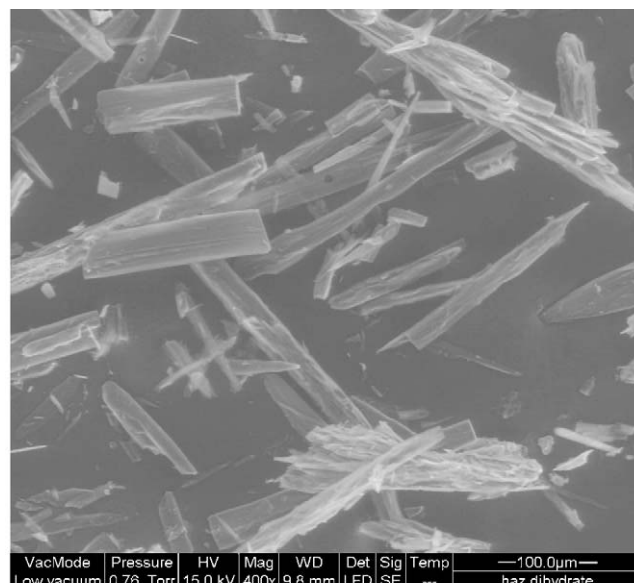


(a)

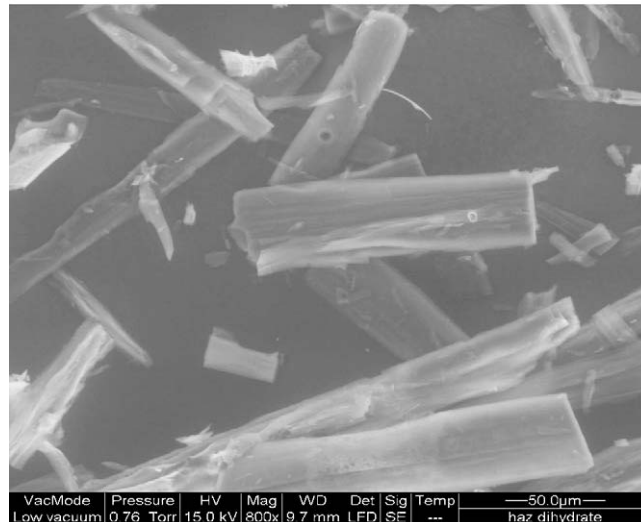


(b)

Fig. 1. (a) SEM image of anhydrous HAZ and (b) SEM image of anhydrous HAZ.



(a)



(b)

Fig. 2. (a) SEM image of anhydrous HAZ dihydrate and (b) SEM image of anhydrous HAZ dihydrate.

ing rates of 5–20 °C min⁻¹. The activation energy for exothermic decomposition of HAZ computed by using ASTM standard method [16] (based on Kissinger correlation) was found to be 136.2 kJ/mol (Table 2). In DSC, single stage exothermic decomposition peak at 188 °C was observed in the case of anhydrous

HAZ (Fig. 4) at a heating rate of 10 °C with heat evolution of 1610 J/g whereas N-DNAT (Fig. 5) decomposed in the range of 163–175 °C with the heat evolution of 1367–1484 J/g at heating rates 5–20 °C. The computed activation energy is 160.7 kJ/mol (Table 3). DATz exothermically decomposed at 132 °C.

Table 2
DSC data on HAZ at various heating rates (Kissinger method)

β (°C)	T_m (K)	T_m^2	$1/T_m$	β/T_m^2	$-\ln(\beta/T_m^2)$	Activation energy (kJ/mol)
5	450	202500	0.002222	2.4691×10^{-5}	10.6091	136.2
10	461	212521	0.002169	4.7054×10^{-5}	9.96421	
15	464	215296	0.002155	6.9672×10^{-5}	9.5717	
20	466	217156	0.002146	9.21×10^{-5}	9.2926	

Table 3
DSC data on N-DNAT at various heating rates (Kissinger method)

β (°C)	T_m (K)	T_m^2	$1/T_m$	β/T_m^2	$-\ln(\beta/T_m^2)$	Activation energy (kJ/mol)
5	436	190096	0.002294	2.6303×10^{-5}	10.5458	160.7
10	445	198025	0.002247	5.0499×10^{-5}	9.89356	
15	447	199809	0.002237	7.5072×10^{-5}	9.4971	
20	448.5	201152	0.00223	9.9427×10^{-5}	9.2161	

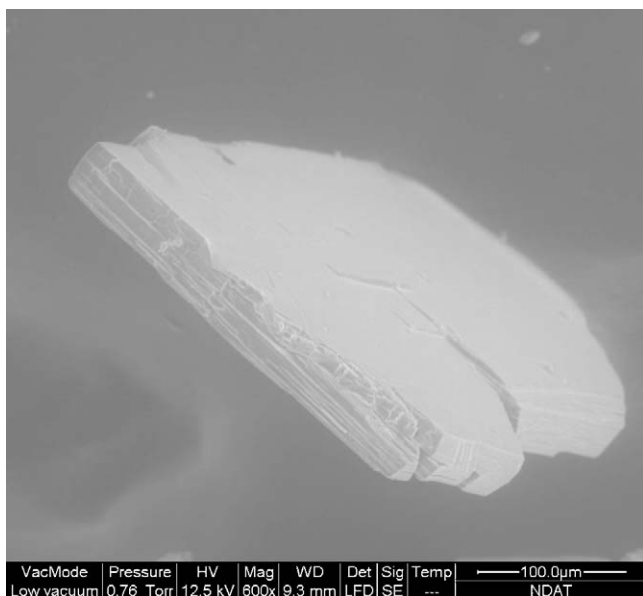


Fig. 3. SEM image of anhydrous N-DNAT.

The TG of HAZ dihydrate (Fig. 6) showed two major weight losses corresponding to 5% loss in weight due to water in the temperature range of 85–105 °C and 77% weight loss due to decomposition of the compound in the temperature range of 150–185 °C. The TG of anhydrous HAZ showed single step decomposition in the temperature range of 150–185 °C with weight loss of 77% (Fig. 6). N-DNAT revealed major decomposition in the temperature range of 160–180 °C with weight loss of 85% (Fig. 7). The FT-IR of decomposition products evolved during TG of HAZ (Fig. 8) displayed bands at $3255\text{--}3261\text{ cm}^{-1}$ for $-\text{NH}$ and $2356\text{--}2358\text{ cm}^{-1}$ for $-\text{C}\equiv\text{N}$ due to the formation of NH_3 and HCN whereas N-DNAT (Fig. 9) showed peaks attributable to HCN , CO and NH_3 .

The decomposition products of the HNC-HEMs have been identified by pyrolysis GC/MS. HNC-HEMs were pyrolyzed at 800 °C and separated with the help of gas chromatography. The separated gaseous products were analyzed by mass spectrometry. HAZ dihydrate showed around eight prominent peaks with m/z values of 14, 15, 16, 17, 18, 26, 27 and 28. The values have been assigned for various gaseous species and presented in Table 3. Gaseous nitrogen (m/z : 28, 100%) is the most prominent one (Fig. 10). Ammonia (NH_3), hydrogen cyanide (HCN),

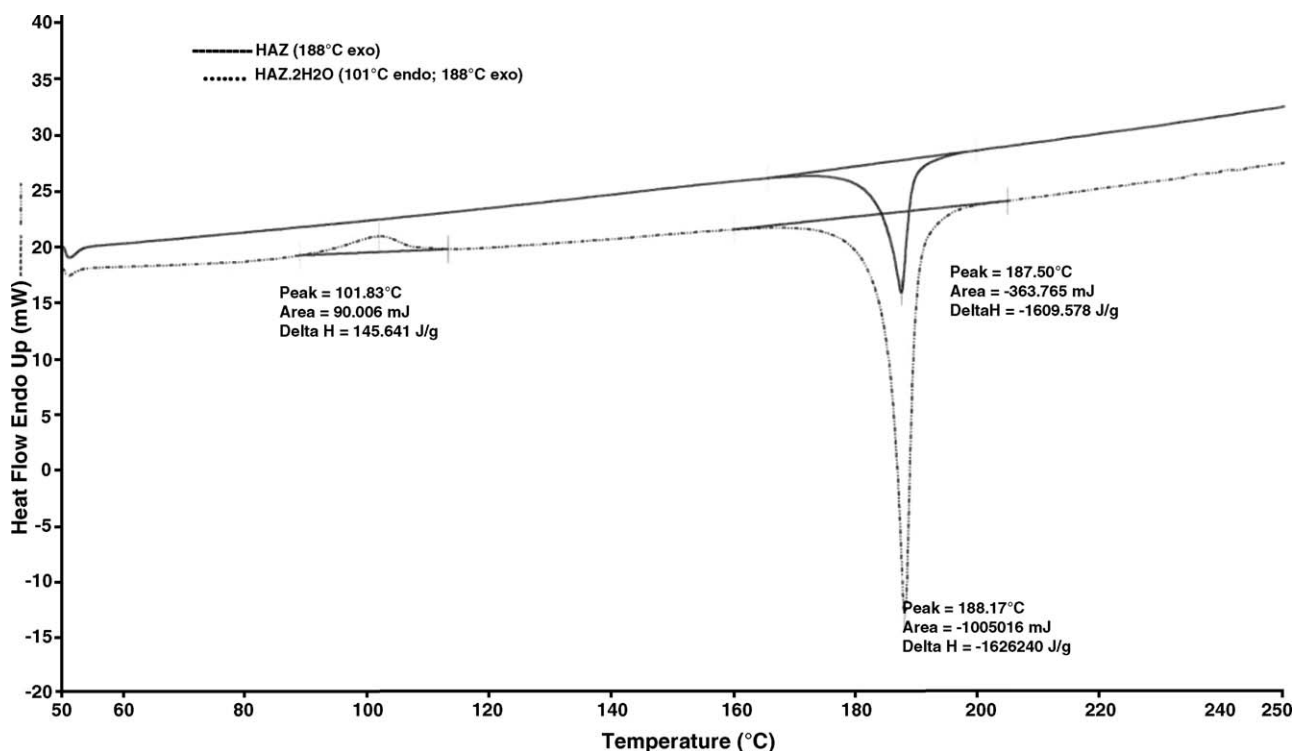


Fig. 4. DSC of anhydrous HAZ and HAZ dihydrate.

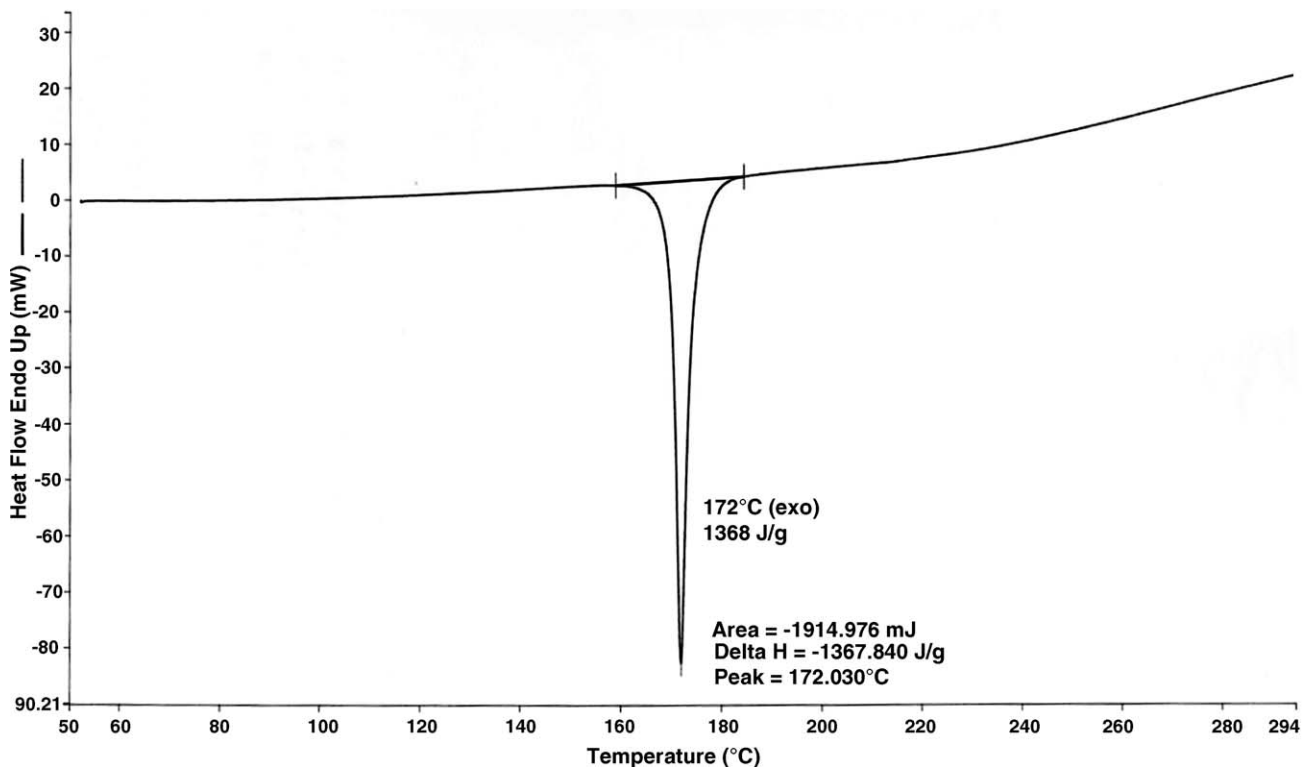


Fig. 5. DSC of N-DNAT.

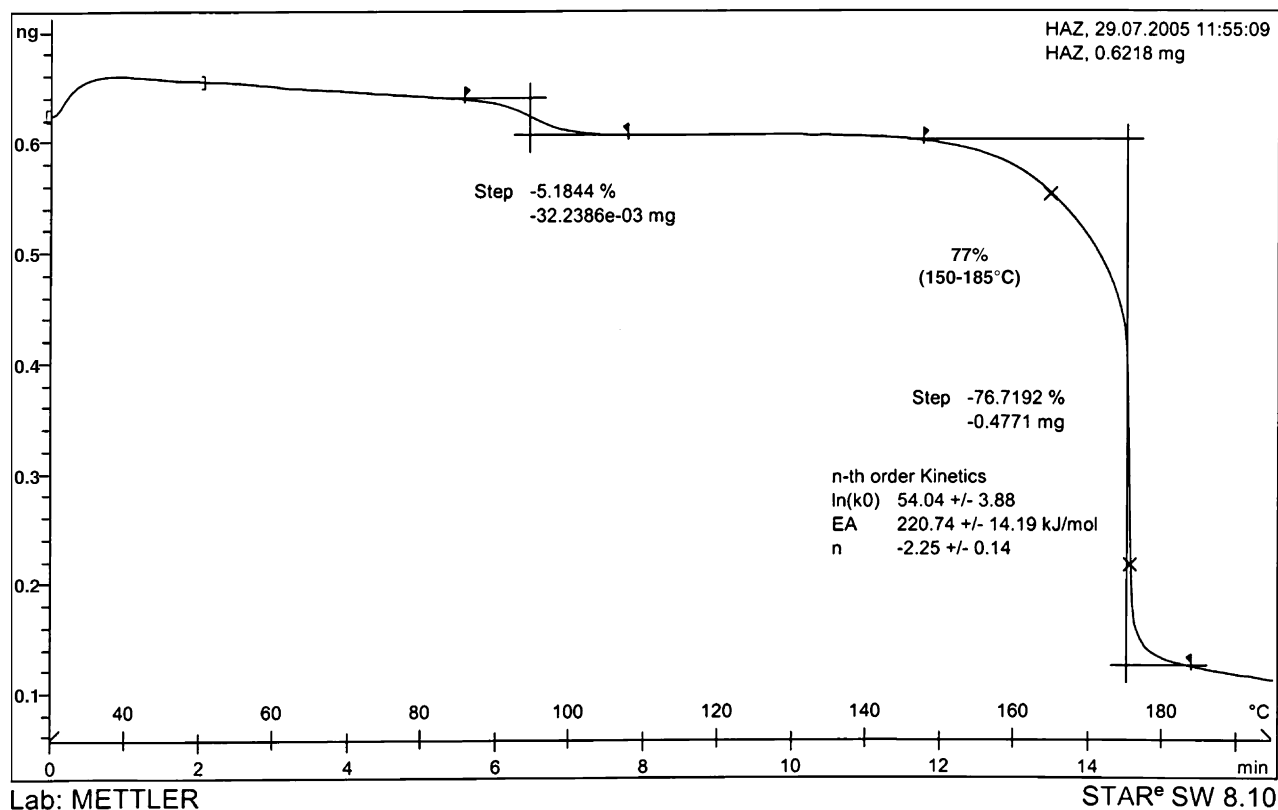


Fig. 6. TG of HAZ dihydrate.

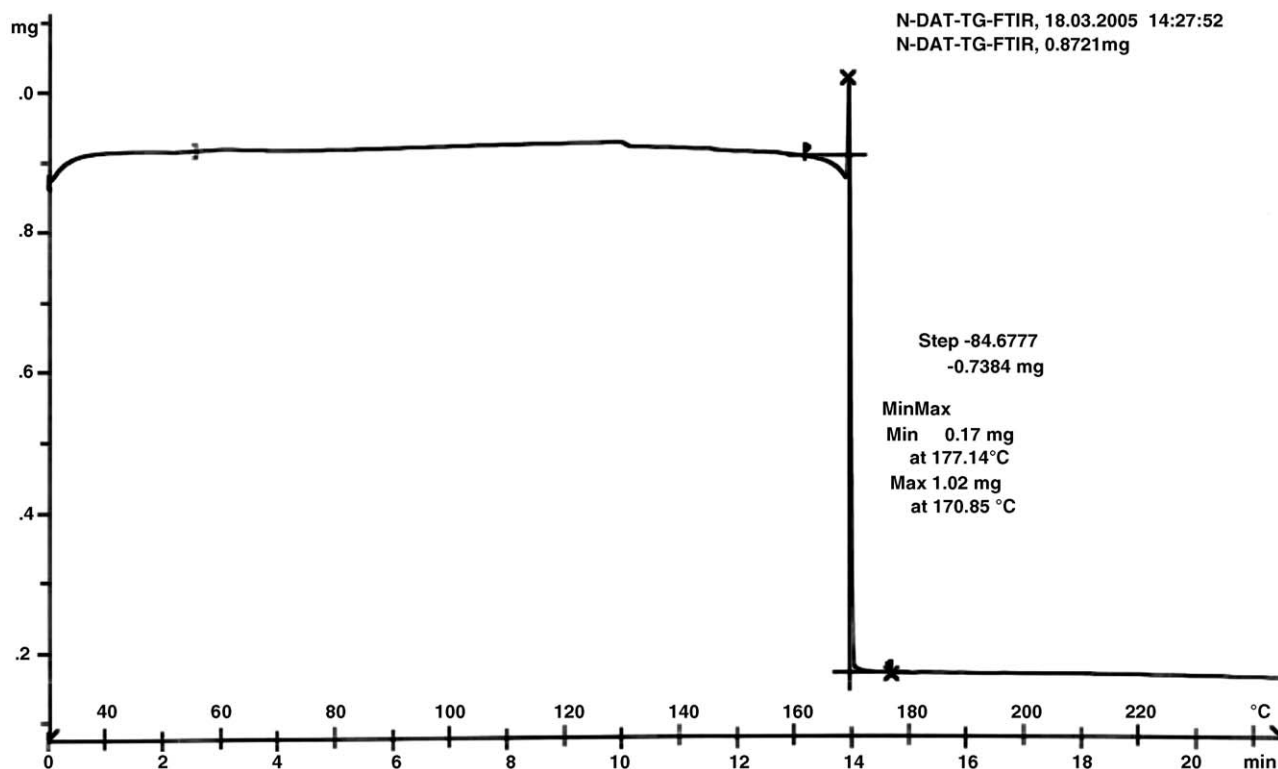


Fig. 7. TG of N-DNAT.

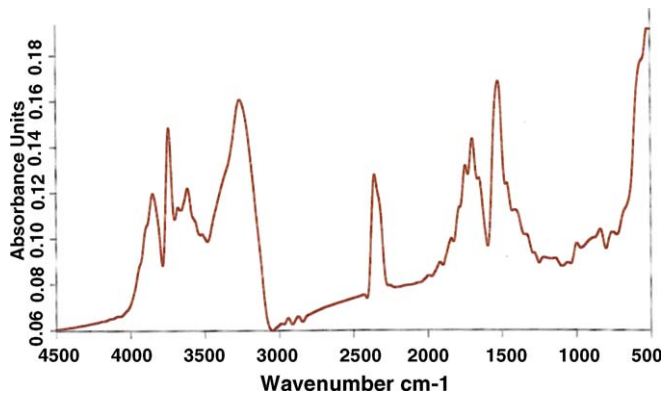


Fig. 8. TG-FT-IR of HAZ.

water (H_2O) and methane (CH_4) are the other prominent gaseous species. The total ion mass spectrum of HAZ dihydrate has been depicted in Fig. 10. Similarly, N-DNAT showed 7 prominent peaks (Table 4) and identified as hydrogen cyanide (HCN), ammonia (NH_3), carbon monoxide (CO), methane (CH_4) and methane related intermediate radical species.

Table 4
Pyrolysed products of HAZ dihydrate and N-DNAT

HAZ								
<i>m/z</i>	14	15	16	17	18	26	27	28
Species	CH_2^\bullet	CH_3^\bullet	CH_4	NH_3	H_2O	CN^\bullet	HCN	N_2
N-DNAT								
<i>m/z</i>	14	15	16	17	26	27	28	
Species	CH_2^\bullet	CH_3^\bullet	CH_4	NH_3	Not present	CN^\bullet	HCN	N_2/CO

Based on the hyphenated TG-FT-IR and pyrolysis GC/MS results, a probable decomposition mechanism has been proposed for HAZ and N-DNAT. It is understood from the results that in the case of HAZ dihydrate, the decomposition commences with rupture of azo linkage between tetrazole rings and with elimination of hydrazinium (N_2H_5^+) as well as water (H_2O). Further, the cleavage of tetrazole ring results in the formation of hydrogen cyanide (HCN) and nitrogen. These gaseous species are undergone recombination and yielded stable gaseous species such as hydrogen, nitrogen and methane (Scheme 4). These results are in good agreement with similar type of compounds previously reported [17]. It is assumed that N-DNAT may also follow similar kind of decomposition pattern. In case of N-DNAT, the decomposition starts with the cleavage of azo linkage between the triazole rings with simultaneous elimination of nitro groups. Further, triazole ring breaks and produces HCN, N_2 and cyanide species (Scheme 5). These species recombine among themselves and produce stable species like H_2 , N_2 and carbon monoxide (CO). The stable species as well as the intermediate species like CO, HCN and N_2 are identified by the hyphenated TG/FT-IR and P-GC/MS techniques.

3.4. Sensitivity studies

The experimentally obtained impact and friction sensitivity of N-DNAT are 22 cm ($\text{H}_{50\%}$ explosion, 2 kg weight) and 8 kg, respectively indicating that N-DNAT is sensitive in nature. HAZ dihydrate is insensitive to impact (>170 cm) as well as friction (up to 36 kg) stimuli whereas the impact and friction sensitivity of anhydrous HAZ are 95 cm and 24 kg, respectively. The results

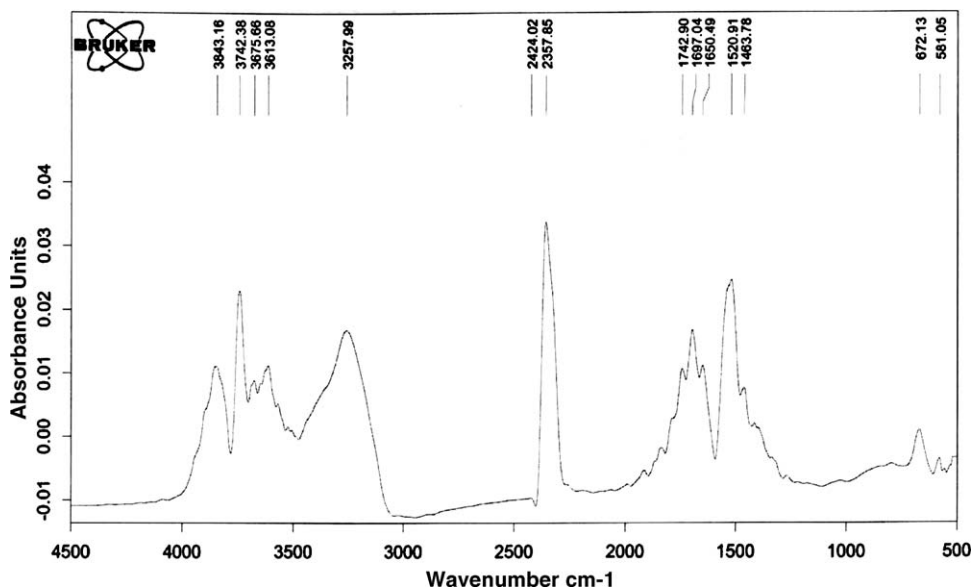


Fig. 9. TG-FT-IR of N-DNAT.

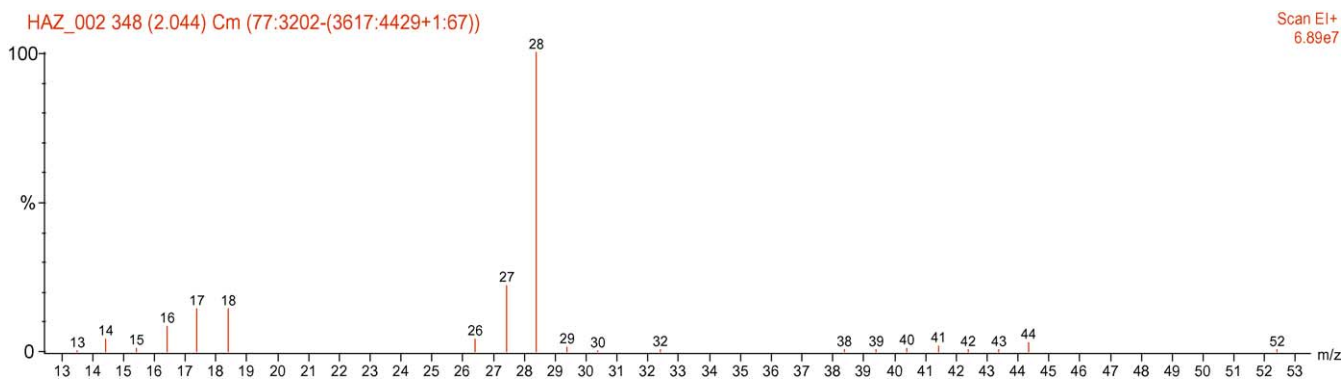
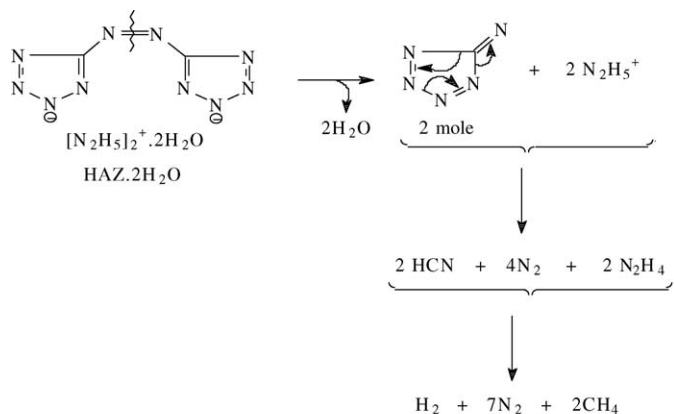
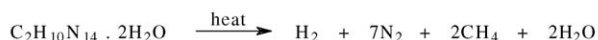


Fig. 10. Py-GC/MS pattern of HAZ.



Overall reaction

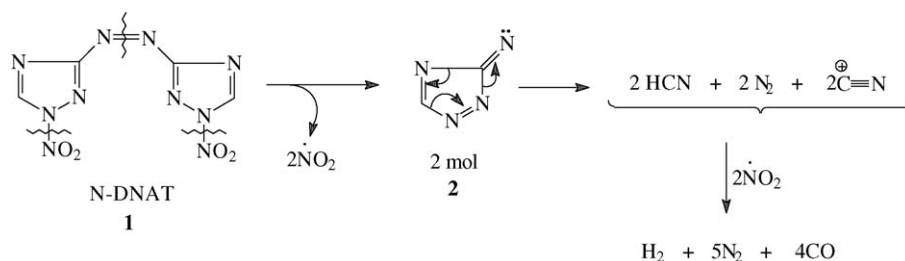


Scheme 4. Decomposition pathway of HAZ dihydrate.

revealed that hydrazinium azotetrazolate dihydrate is insensitive towards impact and friction stimuli compared to anhydrous HAZ.

3.5. Performance evaluation

The theoretical performance data of the HNC-HEMs were generated using the linear output thermodynamic user-friendly software for energetic systems (LOTUSES) [18,19] and are presented in the Table 5. The predicted volume of gaseous products for HAZ is 1436 L/kg of explosive compared to RDX (957 L/kg), which can be used as potential gas generator. The heat of explosion of N-DNAT is 6163 kJ/kg greater than that of RDX (5041 kJ/kg), which can find application as an energetic ingredient in various explosive/propellant formulations. The above results are to be confirmed by generating experimental data by incorporating these ingredients in various formulations. Theoretically computed data revealed that N-DNAT and HAZ can find application in propellant/explosive as well as in gas generator formulations as an energetic ingredient.



Overall reaction



Scheme 5. Decomposition pathway of N-DNAT.

Table 5
Theoretically predicted performance parameters of HNC-HEMs by LOTUSES

Sl. no.	Explosive parameter	HAZ	N-DNAT	RDX	HMX
1	Heat of explosion (kJ/kg)	3743	6163	5041	5018
2	Temperature of explosion (K)	3200	3500	4500	4500
3	Volume of gaseous products (L/kg)	1436	929	957	957
4	Power index (%)	199	114	178	177
5	Relative strength (%)	191	109	171	171
6	Sound intensity (db)	343	373	335	363
7	No. of moles of gaseous products	14	10	9	12
8	Nitrogen content (%)	85	56	37.8	37.8

4. Conclusion

The synthesis and characterization of HAZ and N-DNAT were established during this study. The DSC results showed that hydrazinium azotetrazolate synthesized in the present work is decomposed at 180 °C whereas N-DNAT is stable up to 160 °C. TG-FT-IR studies of these compounds suggest that the presence of NH₃ and HCN in the decomposition products. HAZ and N-DNAT have been subjected for pyrolysis gas chromatography mass spectrometry technique to identify the decomposition gaseous products. It is observed that nitrogen, hydrogen cyanide, methane are the prominent species present in the HNC-HEMs. Based on the thermal study, a probable decomposition pathway has been proposed for both the compounds. Impact and friction test results indicated the sensitive nature of N-DNAT the insensitive nature of HAZ and its dihydrate to impact and friction stimuli. Theoretically predicted detonation performance parameters of HNC-HEMs also discussed.

Acknowledgement

The authors are grateful to A. Subhananda Rao, Director, HEMRL for constant encouragement to carry out this work.

References

- [1] D.E. Chavez, M.A. Hiskey, R.D. Gilardi, *Angew. Chem.* 112 (2000) 1861.
- [2] M. Tremblay, *Can. J. Chem.* 43 (1965) 1154.
- [3] Y.L. Peng, C.W. Wong, US Patent 5,877,300 (March 2, 1999).
- [4] D.E. Chavez, M.A. Hiskey, *J. Energy Mater.* 17 (1999) 357.
- [5] D.E. Chavez, L. Hill, M.A. Hiskey, S. Kinkead, *J. Energy Mater.* 18 (2000) 219.
- [6] S. Lobbecke, A. Pfeil, H.H. Krause, *Propellants Explosives Pyrotechnics* 24 (1999) 168.
- [7] R. Sivabalan, M.B. Talawar, N. Senthilkumar, B. Kavitha, S.N. Asthana, *J. Therm. Anal. Calorim.* 78 (2004) 781.
- [8] M.B. Talawar, R. Sivabalan, N. Senthilkumar, G. Prabhu, S.N. Asthana, *J. Hazmat A113* (2004) 11.
- [9] A. Hammerl, T.M. Klapotke, H. Noth, M. Warchhold, G. Holl, M. Kasier, U. Ticmanis, *Inorg. Chem.* 40 (2001) 3570.
- [10] G. Hammerl, T.M. Holl, P. Klapotke, H. Mayer, H. Noth, M. Piotrowski, Warchhold, *Eur. J. Inorg. Chem.* (2002) 834.
- [11] K.Y. Lee, US Patent 46,623,409A (November 18, 1986).
- [12] J. Thiele, Machot, *Anal. Chem.* 303 (1898) 47.
- [13] K.Y. Lee, *Proceeding of the Working Group Meeting on High Energy Materials*, Dover, NJ, May 22–24, 1984.
- [14] M.V. Huynh, M.A. Hiskey, E.L. Hartline, D.P. Montoya, R. Gilardi, *Angew. Chem. Int. Ed.* 43 (2004) 4924.
- [15] L. Arvani, R. Hutchinson, *The Sensitivity of Impact and Friction: In Energetic Materials—Technology of the Inorganic Azide*, vol. 2, New York, 1977, pp. 111–158.
- [16] ASTM Standard test methods for Arrhenius kinetic constant for thermally unstable materials, Part 41, E698-79, 1982, p. 1012.
- [17] A. Hammerl, G. Holl, T.M. Klapotke, G. Spie, *Internet J. Vib. Spec.* 5 (3) 6 (2001) 1.
- [18] H. Muthurajan, R. Sivabalan, M.B. Talawar, S.N. Asthana, *J. Hazmat.* 117A (2005) 2312.
- [19] H. Muthurajan, R. Sivabalan, M.B. Talawar, M. Anniyappan, S. Venugopalan, *J. Hazmat.* 133 (2006) 30–45.